Tunicate Swarm Algorithm-Based Load Frequency Controller for Renewable Energy Resources Combined Heat Power Network

S. M. ABD ELAZIM
Computer Science Department, College of Engineering and Computer Science,
Jazan University, Jizan,
KINGDOM OF SAUDI ARABIA

Abstract: - Load Frequency Control (LFC) has turned into increasingly complex in various connected energy systems because of rising integration of renewable power resources like photovoltaic (PV) cells plus wind turbines. This work develops an up-to-date fine-tuning technology named the Tunicate Swarm Approach (TSA) for the prime adjusting of a Proportional-Integral-Derivative (PID) controller for LFC. PID tuning challenge of in a robust LFC layout is framed as an optimization issue based on the time-based cost equation that is addressed using the proposed method. TSA has a strong ability to identify the most promising solutions. The block representation of the blend layout is implemented, the simulation outcomes are displayed to evaluate the efficacy of the advised TSA-driven scheme in comparison with Firefly Approach (FA), Genetic Approach (GA), Ant Lion Optimization (ALO), and Water Cycle Approach (WCA). These outcomes demonstrate that the suggested controller performs more efficient than the others when analysing time-domain characteristics and various performance metrics.

Key-Words: - TSA, LFC, PID, ITAE, Two areas System, Renewable Energy.

Received: May 11, 2024. Revised: November 3, 2024. Accepted: December 6, 2024. Published: February 3, 2025.

1 Introduction

The primary goal of Load Frequency Control (LFC) is to maintain inter-area grid tie energy along with frequencies throughout acceptable limits in response to disturbances and load variations, [1]. This objective is crucial for LFC because a well-designed electrical network can sustain voltage and frequency levels within specified boundaries while maintaining overall system performance, [2].

Various methods have been applied to LFC design, including robust control [3], [4], decentralized control [5], linear quadratic regulation [6], pole shifting [7] and adaptive control [8]. However, these methods have various drawbacks that limit their effectiveness. To overcome these challenges, several studies have explored artificial intelligence strategies like Fuzzy Logic (FL) [9], [10] plus Neural Networks (NN) [11]. While the effective of these techniques at managing the nonlinearity in the power system, they also come with limitations, they also have limitations. For instance, Neural Networks can be challenging to configure due to the need to determine the number of neurons and layers, while Fuzzy Logic requires significant effort to identify the appropriate input variables. The second approach involves using the Evolutionary Approach (EA), which is effective in managing the LFC process due to its capability to solve complex Non-uniform equations. Techniques such as the Genetic Algorithm (GA) [12], Bacteria Foraging [13], [14], Gravitational Search [15], Cuckoo Search [16], Particle Swarm Optimization (PSO) [17], [18], Firefly approach [19], Differential Evolution (DE) [20], Marine Predator Algorithm [21], Bat Algorithm [22], Crow Search [23], [24], Ant-Lion Optimizer (ALO) [25], [26], and Whale Optimization Algorithm [27], [28], [29], [30] have been deployed in the LFC layout. Even so these schemes appear useful for the plan problem, they suffer from lagging converging behaviour and limited regional optimization capabilities, which can lead them to become trapped in localized minima.

The Tunicate Swarm Algorithm (TSA) is an up-to-date metaheuristic and population-based optimization tool which imitates tunicate jet-forced motion and swarming performances throughout navigation and foraging. It is particularly effective for fixing restricted optimization challenges and is more dynamic compared to other population and stochastic-based approaches previously discussed, [31]. TSA-tuned controller parameters have been applied in various contexts [32], [33], [34], [35], demonstrating greater robustness and superior stabilization. However, the utilization of TSA in LFC has not yet been explored in recent studies. Its ability to balance exploration and exploitation phases has inspired researchers to use TSA for optimizing PID-based LFC problems in this article.

This article introduces a new optimization algorithm, TSA, designed to identify the best PID-LFC constants to a heat grid connected along a photovoltaic system. This work intends to prove the TSA-PID effectiveness and to enhance the stability of grid tie power and frequency fluctuations under various situations.

2 Heat Grid Configuration

Zone 1 represents a heat grid that includes a turbine, supply, reheater, and governor. The parameters of the network under study are detailed in the appendix. The equations for the various transfer functions are provided below, [36]:

The equalization for the governor is expressed as:

$$\frac{K_{go}}{T_{go}\,S+1} \quad (1)$$

The equalization for the reheater is expressed as:

$$\frac{K_{re}\,T_{re}\,S+1}{T_{re}\,S+1} \quad (2)$$

The equalization for the thermal turbine is expressed by:

$$\frac{K_{tu}}{T_{tu}\,S+1} \quad (3)$$

and the equalization for the dynamo is expressed as:

$$\frac{K_d}{T_d\,S+1} \quad (4)$$

In this zone, the Area Control Error (ACE) signals, which consist of deviations in frequencies along with grid tie-in energy, can be expressed as:

$$ACE_n = B.\Delta f_n + \Delta P_{Tie} \quad (5)$$

3 PV Model

The PV grid layout consists of a photovoltaic power supply that is in direct correlation to daylight strength, connected in alongside a small series resistance plus a diode, as illustrated in Figure 1. The output current and voltage from the cell correspond to the running conditions of the load. The arithmetic representation of the photovoltaic cell is expressed by the upcoming formulas, [19].

$$I_c = I_{ph} - I_o\left\{e^{\left[\frac{q_o}{AKT}\left(V_c + I_c R_s\right)\right]} - 1\right\} \quad (6)$$

$$V_c = \frac{AKT}{q_o}\ln\left(\frac{I_{ph}+I_o-I_c}{I_o}\right) - I_c R_s \quad (7)$$

$$I = I_{ph} - I_o\left\{e^{\left[\frac{q_o}{n_s AKT}\left(V + n_s I R_s\right)\right]} - 1\right\} \quad (8)$$

$$V = \frac{n_s AKT}{q_o}\ln\left(\frac{I_{ph}+I_o-I}{I_o}\right) - n_s I R_s \quad (9)$$

where;

$$I_{ph} = \frac{G}{1000}\left[I_{sc} + k_i\left(T - T_r\right)\right] \quad (10)$$

$$I_o = I_{or}\left(\frac{T}{T_r}\right)^3 e^{\left[\frac{q_o E_g}{AK}\left(\frac{1}{T_r} - \frac{1}{T}\right)\right]} \quad (11)$$

The output power of the model can be directly determined using the upcoming formula.

$$P = I.V \quad (12)$$

While,

I, V	Model generated current as well as potential.
I_c, V_c	Cell product current as well as potential.
I_s	The revert cell maximum capacity current
I_{ph}, V_{ph}	Light-generated voltage and current.
K	Boltzmann ratio.
I_{sc}	Short circuit current.
I_o	Revert saturation current.
R_s	The series resistance.
T	Cell heat,
E_g	Silicon energy gab.
q_o	Electrical charge.
KT	Heat ratio (0.0017 A/C°).
G	The solar irradiance in W/m[2.]

A	Idealist element.
T_r	The referred temperature,
I_{or}	The saturation current rating of cell at T_r,
n_s	The number of photovoltaic cells connected in series.
k_i	The cell heat constant.

Therefore, once the model constants, including I_o, R_s and A, are determined, current-potential curve for PV model is given by formulas (8 and 9).

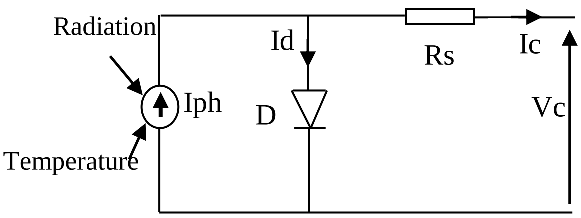

Fig. 1: Model of PV cell

To maximize the output power from a solar grid, it is essential to work at the peak energy point. The solar grid productivity is influenced by aspects for instance temperature and irradiation. The MPPT approach is used to enhance the system effectiveness.

The PV model including filter, MPPT, and inverter is described by the upcoming formula [36]:

$$G_{PV} = \frac{-18S + 900}{S^2 + 100S + 50} \tag{13}$$

The block graph of the network under consideration is depicted in Figure 2 (Appendix). Variations in temperature and radiation are mapped as unit stage functions in the solar grid.

4 Optimization Process

In the considered network, the traditional integral block can be replaced with a PID block as described by the upcoming equalization:

$$k_n(S) = k_{Pn} + \frac{k_{In}}{S} + Sk_{Dn} \tag{14}$$

The control input is represented by the equalization:

$$U_n(S) = -k_n(S)\ ACE_n(S). \tag{15}$$

A specific performance measure can be achieved using the Integral of Time times Absolute Error (ITAE) of frequencies variations in two zones and the grid tie power. Consequently, the cost equation is formulated as:

$$J = \int_0^\infty t\left(\left|\Delta f_1\right| + \left|\Delta P_{Tie}\right| + \left|\Delta f_2\right|\right)dt \tag{16}$$

To improve operational performance, it is crucial to lessen equation (16). The optimization job can be modelled as a bounded minimization task while:

$$k_{Pn}^{lower} \le k_{Pn} \le k_{Pn}^{upper},$$
$$k_{In}^{lower} \le k_{In} \le k_{In}^{upper},$$
$$k_{Dn}^{lower} \le k_{Dn} \le k_{Dn}^{upper} \tag{17}$$

The selected values borders are [-2 to 2], as indicated in [19], [26] and the designed cost function is evaluated with a 0.1 trouble in each zone.

5 Tunicate Swarm Approach

The tunicate swarm optimization procedure is a population-focused swarm process recommended to fix large-scale optimization tasks. Tunicates exhibit radiant bioluminescence, emitting a dim blue/green glow perceptible from several meters away [31]. As every tunicate measure just a little millimetre long, sharing a collective gel-like sheath, the entire tunicates are tied together. Moreover, every tunicate individually extracts the moisture and generate the jet force through its unsealed terminal using atrial channels. Tunicate changes its present location with a propulsion-motivated liquid jet. This propulsion migrates the tunicates uprightly into the ocean depths. The prime impressive attributes of tunicate are their jet propulsion and swarm responses, [32].

TSA utilizes the location of the finest tunicate of the community for the target of refining the tunicate diversification and intensification. Thus, the opportunity of discovering a superior location for seek engines has intensified. Even though tunicate has no clue what the food source integrity is, it has the capability to locate the food sources in the deep blue. Tunicate employs Jet propulsion and swarming behavioral models to reach the food resource. Tunicate has triple attitudes throughout Jet propulsion attitude, [33]. These attitudes are; preventing disputes within the community of the tunicate throughout the searching trip that every tunicate regularly attempts to organize itself toward the highly finest individual and aims to stay close to the best individual. To avoid disputes within tunicates, the agent A is employed to locate the up-to-date location of the present tunicate, and it is processed based on the formulas provided beneath:

$$\vec{a} = \vec{g}/\vec{m} \tag{18}$$

$$\vec{g} = C_2 * C_3 - \vec{f} \tag{19}$$

$$\vec{f} = 2.C_1 \tag{20}$$

where, $\vec{g}$ points to gravitational attraction and $\vec{f}$ points to stream direction in the sea.

$C_1, C_2 and\, C_3$ points to a haphazard true amount developed in the span from 0 to 1. The agent $\vec{M}$is declared as the social strength via tunicates (search engines) in the area under search and computed via formula (21).

$$\vec{m} = \{P_{MIN} + C_1.(P_{MAX} - P_{MIN})\} \tag{21}$$

Hence, P_{MIN} and P_{MAX} are primary and subsequent movement rate for social engagement, and these amounts are taken as 1 and 4, correspondingly [34]. Afterward disputes among neighboring tunicates are avoided, search engines start to head toward the neighboring tunicate that has the prime fitness amount. The motion of the current tunicate to the finest tunicate is computed by formula (22):

$$\vec{Pd} = [\vec{Fs} - r_{rand}.\vec{P_p}(X)] \tag{22}$$

Hence, $\vec{Pd}$ indicates gap within the search engine and food resource, X denotes present loop, $\vec{Fs}$ is location of the tunicate gaining the prime performance amount, $\vec{P_p}$(X) is location of the current individual, and r_{rand} points to a haphazard true amount developed in the span of [0,1]. The updated location of $\vec{P_p}$(X') is computed by formula (23).

$$\vec{Pd} = \begin{Bmatrix} \vec{Fs} + \vec{A}.\vec{P}, if\ r_{rand} \geq 0.5 \\ \vec{Fs} - \vec{A}.\vec{P}, if\ r_{rand} < 0.5 \end{Bmatrix} \tag{23}$$

$\vec{P_p}$(X') refers to the updated location generated for $\vec{P_p}$(X) related to the location of the prime food resource $\vec{FS}$. The arithmetic layout of the swarming configuration for tunicates is illustrated by formula (24); the initial two prime optimal outcomes are stored; the left search engine's locations modified along with the position of the stored prime outcomes.

$$\vec{P_p}\,(X+1) = \frac{\vec{P_p}\,(X) + \vec{P_p}\,(X+1)}{C_1+2} \tag{24}$$

After location upgrade procedure, tunicate newest location yield to a random one, with a tube-like or cone structure. $\vec{A}$, $\vec{G}$ and $\vec{F}$ support the position of tunicates to shift haphazardly in a particular search area and prohibit the tunicate population disputes. The capability of TSA exploitation and exploration are presented by vectors$\vec{A}$, $\vec{G}$and $\vec{F}$. The TSA flowchart for fixing LFC issue is presented in Figure 3 (Appendix). It is agreed from Figure 3 (Appendix), initially, the TSA is launched with direct elements. Then, the remains TSA stages are carried out to fix the LFC issue. lastly, the tunicate location where the prime performance amount is recorded.

6 Outcomes and Emulations

Various events are tested to ensure the effectiveness of the TSA method for selecting optimal PID values. The TSA [32] was implemented in MATLAB 7.1. The results demonstrate that this approach is superior to others based on a range of metrics. Table 1 illustrates the performance of every controller and different indicators values.

6.1 Case 1: Load Stage Variation in the Heat Network

A 0.1 shift raise in the thermal grid requirement is applied. Figure 4, Figure 5 and Figure 6 display outcomes. Obviously suggested PIDs yield better results in alleviating stabilization phenomena of electric network regarding ALO, WCA, FA, and GA. Consequently, TSA demonstrates better performance than the other methods.

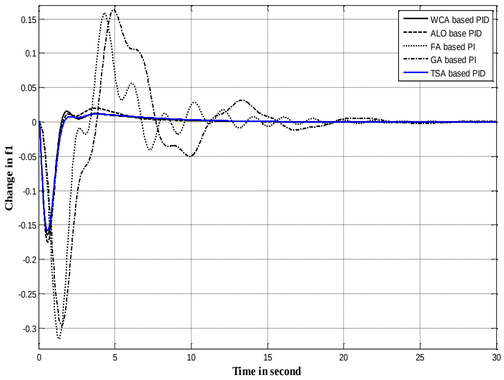

Fig. 4: Change in f_1 for case 1

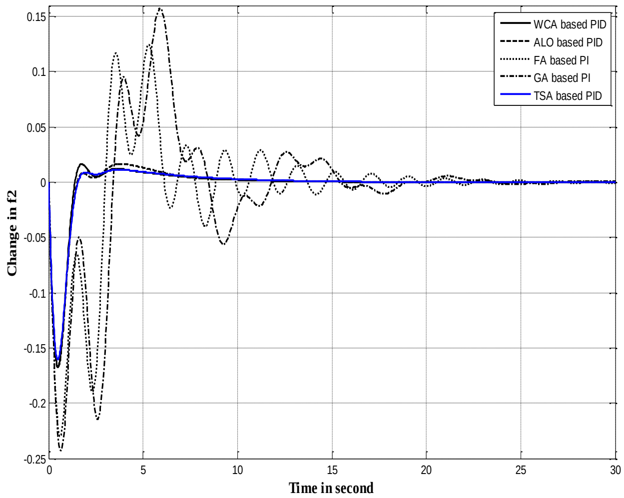

Fig. 5: Variation of f_2 in case 1

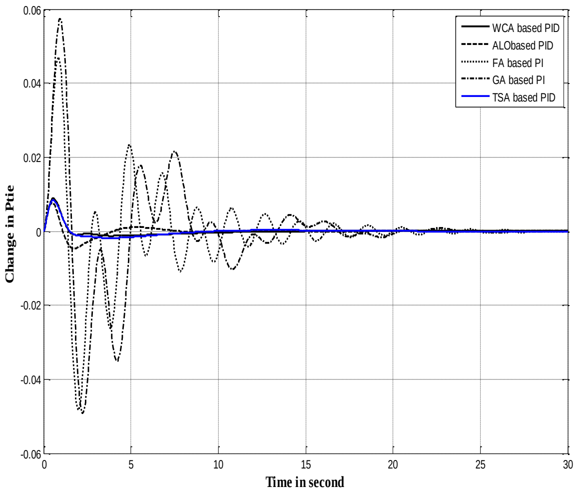

Fig. 6: P_{Tie} Change for the first scenario

6.2 Case 2: Shift Variation in Dual Zones

In this strategy, a 0.1 shift increment is applied to the load of the heat grid, temperature, radiation, and solar grid. Figure 7, Figure 8 and Figure 9 illustrate the outcomes. In these figures, the network fluctuations are reduced using the suggested PIDs. Additionally, the developed PIDs demonstrate a shorter settling time compared to ALO, FA, WCA, and GA, and the network quickly reaches a stable condition. This highlights efficacy of the approach in addressing LFC issue.

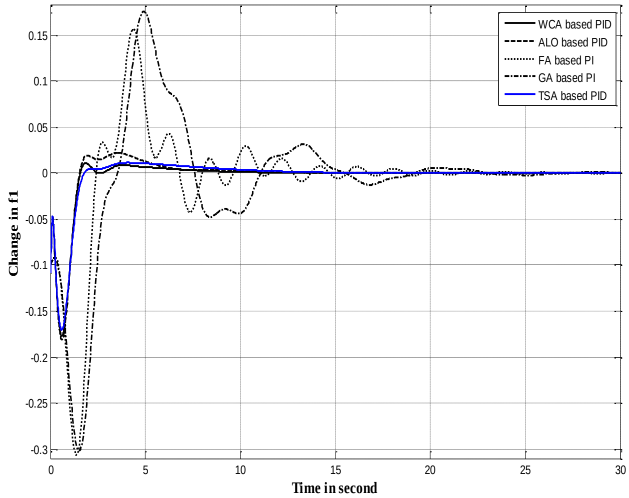

Fig. 7: Change in f_1 for the second scenario

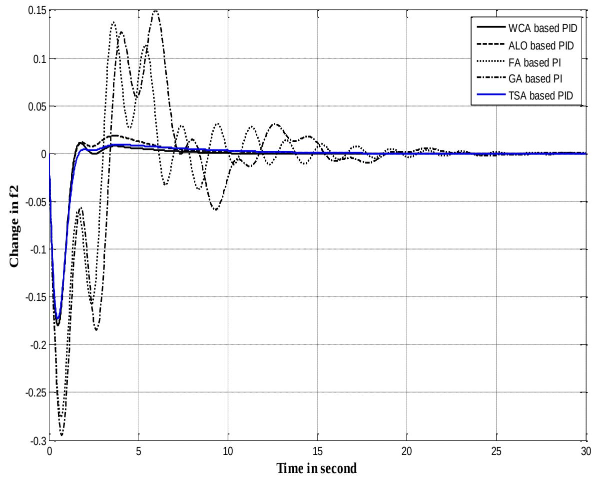

Fig. 8: Change in f_2 for the second scenario

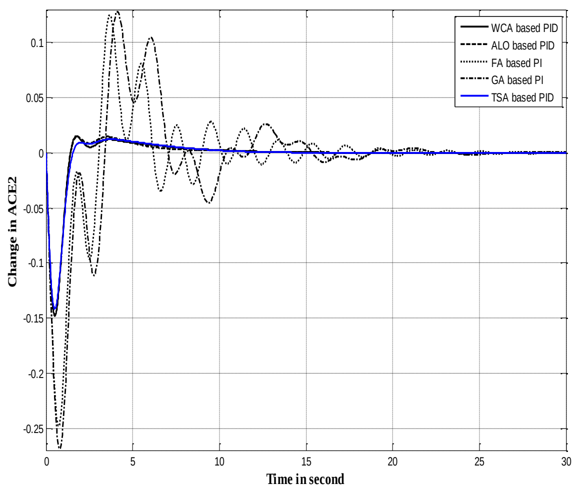

Fig. 9: ACE_2 variation for the second scenario

6.3 Performance Indicators and Robustness

The efficacy of the developed PIDs is validated via several indicators like Integral of Absolute Error (IAE), Integral of Time-weighted Absolute Error (ITAE), Integral of Squared Error (ISE), and Integral of Time-weighted Squared Error (ITSE):

$$IAE=\int_0^{30}\left(\left|\Delta f_1\right|+\left|\Delta P_{Tie}\right|+\left|\Delta f_2\right|\right)dt \tag{25}$$

$$ITAE=\int_0^{30} t\left(\left|\Delta f_1\right|+\left|\Delta P_{Tie}\right|+\left|\Delta f_2\right|\right)dt \tag{26}$$

$$ISE=\int_0^{30} (\Delta f_1^2+\Delta f_2^2+\Delta P_{Tie}^2)\,dt \tag{27}$$

$$ITSE=\int_0^{30} t\left(\Delta f_1^2+\Delta f_2^2+\Delta P_{Tie}^2\right)dt \tag{28}$$

Table 1 lists the constants for each PID compared with [19], [26], as Table 2 displays the amount of the different indicators. It is obvious that the amount of these indicators for the developed PIDs are less relative to those of WOA [37], MWOA [37], SHO [37], FA [19], and GA [19]. This indicates that the time-based attributes are significantly improved by applying the developed TSA. Therefore, the regulators optimized through TSA are more robust and more rapid than the others.

Table. 1. The constants of various approaches

PID Values	FA based PI [19]	GA based PI [19]	ALO based PID [26]	**TSA**
k_{P1}	-0.8811	-0.5663	-1.999	**-0.9217**
k_{I1}	-0.5765	-0.4024	-1.973	**-0.291**
k_{D1}	-0.7626	-0.5127	-1.9953	**-1.9811**
k_{P2}	-0.8307	-0.7256	-2	**-1.994**
k_{I2}			-2	**-1.94**
k_{D2}			-1.4618	**-0.3285**

7 Conclusions

This article determines the optimal PID constants for LFC through the use of TSA. The solar grid, operating at MPPT, is incorporated into the heat grid. A developed charge equalization method is used to improve network response by integrating the time absolute error of frequency changes across interconnected zones and grid tie power. The effectiveness of the suggested scheme is validated by applying multiple metrics and interruptions. It is evident that TSA operates superior to ALO, FA, WCA, and GA in managing the LFC process. Additionally, the supremacy of the recommended PID controllers is confirmed by the assessment of different indicators.

Table. 2. The performance indices for various approaches.

Algorithm	IAE	ITAE	ISE	ITSE
GA adjusted PI [19]	2.334	12.124	0.320	0.862
FA adjusted PI [19]	1.721	7.426	0.291	0.472
WOA adjusted PI [37]	1.057	4.121	0.166	0.426
SHO adjusted PI [37]	0.649	2.531	0.102	0.2618
MWOA adjusted PID [37]	0.563	1.560	0.086	0.060
SHO adjusted PID [37]	0.309	0.858	0.045	0.037
Proposed TSA	**0.277**	**0.732**	**0.04**	**0.030**

Declaration of Generative AI and AI-assisted Technologies in the Writing Process

While preparing this work, the authors used Grammarly to edit the language. After using this service, the author reviewed and edited the content as needed and took full responsibility for the content of the publication.

References:

[1] H. Bevrani, *Robust Power System Frequency Control,* Switzerland, 2nd Edition, Springer, 2014, https://doi.org/10.1007/978-0-387-84878-5.

[2] H. J. Lee, J. B. Park, and Y. H. Joo, “Robust Load-Frequency Control for Uncertain Nonlinear Power Systems: A Fuzzy Logic

Approach", *Int. J. of Information Sciences*, Vol. 176, No. 23, 2006, pp. 3520-3537, https://doi.org/10.1016/j.ins.2006.01.003.

[3] W. Tan, and Z. Xu, "Robust Analysis and Design of Load Frequency Controller for Power Systems", *Electric Power Systems Research*, Vol. 79, Issue 5, May 2009, pp. 846-853, https://doi.org/10.1016/j.epsr.2008.11.005.

[4] W. Tan, and H. Zhou, "Robust Analysis of Decentralized Load Frequency Control for Multi-Area Power Systems", *Int. J. of Electrical Power and Energy Systems*, Vol. 43, Issue 1, Dec. 2012, pp. 996-1005, https://doi.org/10.1016/j.ijepes.2012.05.063.

[5] S. Selvakumaran, S. Parthasarathy, R. Karthigaivel and V. Rajasekaran, "Optimal Decentralized Load Frequency Control in a Parallel AC-DC Interconnected Power System Through HVDC Link Using PSO Algorithm", *Energy Procedia*, Vol. 14, 2012, pp. 1849-1854, https://doi.org/10.1016/j.egypro.2011.12.1178.

[6] S. K. Pandey, S. R. Mohanty, N. Kishor, and J. P. S. Catalão, "An Advanced LMI-Based-LQR Design for Load Frequency Control of an Autonomous Hybrid Generation System", Technological Innovation for the Internet of Things, *IFIP Advances in Information and Communication Technology*, Vol. 394, 2013, pp. 371-381, https://doi.org/10.1007/978-3-642-37291-9_40.

[7] N. Hasan, "Design and Analysis of Pole-Placement Controller for Interconnected Power Systems", *Int. J. of Emerging Technology and Advanced Engineering*, Vol. 2, Issue 8, Aug. 2012, pp. 212-217, [Online]. https://www.semanticscholar.org/paper/Design-and-Analysis-of-Pole-Placement-Controller-Hasan/5e2fbc317a0b176998d3e8ec6858dd06e374b77c?utm_source=direct_link (Accessed Date: December 15, 2024).

[8] N. N. Bengiamin and W. C. Chan, "Variable Structure Control of Electric Power Generation", *IEEE Trans. Power Appar. Syst.*, PAS-101, 1982, pp. 376-380, DOI: 10.1109/TPAS.1982.317117.

[9] M. A. Zamee, D. Mitra, and S. Y. Tahhan, "Load Frequency Control of Interconnected Hydro-Thermal Power System Using Conventional PI and Fuzzy Logic Controller", *Int. J. of Energy and Power Engineering*. Vol. 2, No. 5, 2013, pp. 191-196, DOI: 10.11648/j.ijepe.20130205.12.

[10] H. A. Yousef, K. AL-Kharusi, M. H. Albadi, and N. Hosseinzadeh, "Load Frequency Control of a Multi-Area Power System: An Adaptive Fuzzy Logic Approach", *IEEE Trans. on Power Systems*, Vol. 29, Issue 4, 2014, pp.1822 -1830, DOI: 10.1109/TPWRS.2013.2297432.

[11] R. Francis, and I. A. Chidambaram, "Application of Modified Dynamic Neural Network for the Load Frequency Control of a Two Area Thermal Reheat Power System", *Int. Review of Automatic Control*, Vol. 6, No. 1, 2013, pp. 47-53, [Online]. http://www.praiseworthyprize.org/jsm/index.php?journal=ireaco&page=article&op=view&path%5B%5D=10692 (Accessed Date: December 15, 2024).

[12] V. Jeyalakshmi, and P. Subburaj, "Load Frequency Control in Two Area Multi Units Interconnected Power System Using Multi objective Genetic Algorithm", *WSEAS Trans. on Power Systems*, 2015, Vol. 10, pp. 35-45, [Online]. https://wseas.com/journals/articles.php?id=4488 (Accessed Date: December 15, 2024).

[13] E. S. Ali, and S. M. Abd-Elazim, "Bacteria Foraging Optimization Algorithm Based Load Frequency Controller for Interconnected Power System", *Int. J. of Electrical Power and Energy Systems*, Vol. 33, No. 3, March 2011, pp. 633-638, https://doi.org/10.1016/j.ijepes.2010.12.022.

[14] S. S. Dhillon, J. S. Lather, and S. Marwaha, "Multi Objective Load Frequency Control Using Hybrid Bacterial Foraging and Particle Swarm Optimized PI Controller", *International Journal of Electrical Power & Energy Systems*, Vol. 79, July 2016, pp. 196-209, DOI: doi.org/10.1016/j.ijepes.2016.01.012.

[15] S. J. Safi, S. S. Tezcan, I. Eke, and Z. Farhad, "Gravitational Search Algorithm (GSA) Based PID Controller Design for Two Area Multi-Source Power System Load Frequency Control (LFC)", Gazi University, *J. of Science*, 2018, Vol. 31, No. 1, pp.139-153, [Online]. https://www.researchgate.net/publication/330998943_Gravitational_search_algorithm_GSA_based_PID_controller_design_for_two_area_multi-source_power_system_load_frequency_cont

rol_LFC (Accessed Date: December 15, 2024).

[16] A. Y. Abd-Elaziz and E. S. Ali, "Load Frequency Controller Design via Artificial Cuckoo Search", *Electric Power Components and System*, Vol. 44, Issue 1, 2016, pp. 90-98, https://doi.org/10.1080/15325008.2015.1090502.

[17] V. G. Babu, B. Hemanth, T. S. Kumar and B. V. Prasanth, "Single Area Load Frequency Control Problem Using Particle Swarm Optimization", *Int. J. of Engineering and Science*, Vol. 3, No. 6, 2014, pp. 46-52, [Online]. https://www.theijes.com/papers/v3-i6/Version-2/G0362046052.pdf (Accessed Date: December 15, 2024).

[18] K. Jagatheesan, B. Anand and M.A. Ebrahim**,** "Stochastic Particle Swarm Optimization for Tuning of PID Controller in Load Frequency Control of Single Area Reheat Thermal Power System", *Int. J. of Electrical and Power Engineering*, Vol. 8, No. 2, 2014, pp. 33-40, [Online]. https://www.researchgate.net/publication/271767460_Stochastic_Particle_Swarm_Optimizaion_for_Tuning_of_PID_Controller_in_Load_Frequency_Control_of_Single_Area_Reheat_Thermal_Power_System (Accessed Date: December 15, 2024).

[19] S. M. Abd-Elazim, and E. S. Ali, "Firefly Algorithm-based Load Frequency Controller design of a Two Area System Composing of PV Grid and Thermal Generator", Electrical Engineering, Vol.100, No. 2, June 2018, pp.1253-1262, https://doi.org/10.1007/s00202-017-0576-5.

[20] N. Jalali, H. Razmi, H. D. Mojarrad, "Optimized Fuzzy Self-Tuning PID Controller Design based on Tribe-DE Optimization Algorithm and Rule Weight Adjustment Method for Load Frequency Control of Interconnected Multi-area Power Systems", *J . Applied Soft Computing*, 2020, Vol. 93, 106424, https://doi.org/10.1016/j.asoc.2020.106424.

[21] A. H. Yakout, H. Kotb, H. M. Hasanien, and K. M. Aboras, "Optimal Fuzzy PIDF Load Frequency Controller for Hybrid Microgrid System Using Marine Predator Algorithm", *IEEE Access*, 2021, Vol. 9, pp. 54220-54232, https://doi.org/10.1109/ACCESS.2021.3070076.

[22] S. M. Abd-Elazim, and E. S. Ali, "Load Frequency Controller Design via BAT Algorithm for Nonlinear Interconnected Power System", *Int. J. of Electrical Power and Energy Systems*, Vol. 77C, May 2016, pp. 166-177, https://doi.org/10.1016/j.ijepes.2015.11.029.

[23] N. R. Babu, L. C. Saikia, S. Bhagat, and A. Saha, "Maiden Application of Hybrid Crow-Search Algorithm with Particle Swarm Optimization in LFC Studies", In: P. Bansal, M. Tushir, V. Balas, and R. Srivastava, (Eds) *Proceedings of Int. Conference on Artificial Intelligence and Applications; Advances in Intelligent Systems and Computing*, Vol. 1164. Springer, Singapore 2021, pp. 427-439, https://doi.org/10.1007/978-981-15-4992-2_40.

[24] N. R. Babu, L. C. Saikia, S. K. Bhagat, S. K. Ramoji, B. Dekaraja, and M. K. Behra, "LFC of a Solar Thermal Integrated Thermal System Considering CSO Optimized TI-DN Controller", In: B. Das, R. Patgiri, S. Bandyopadhyay, and V. E. Balas ,(Eds) *Modeling, Simulation and Optimization. Smart Innovation, Systems and Technologies*. Springer, Singapore, 2021, pp. 323-334, https://doi.org/10.1007/978-981-15-9829-6_25.

[25] N. C. Patel, B. K. Sahu, D. P. Bagarty, P. Das, and M. K. Debnath, "A Novel Application of ALO-based Fractional Order Fuzzy PID Controller for AGC of Power System with *Diverse Sources of Generation*", *Int. J. of Electrical Engineering Education*, 2021, Vol. 58, pp.465-487, https://doi.org/10.1177/0020720919829710.

[26] O. Can, A. Ozturk, and H. Kotb, "Ant-Lion Optimizer-Based Load Frequency Controller for a Hybrid Power System with PV and Thermal Power Plant", *Research Square*, June 29th, 2022, https://doi.org/10.21203/rs.3.rs-1669336/v1.

[27] D. Mohanty, and S. Panda, "Frequency control of Hybrid Power System by Sine Function Adapted Improved Whale Optimization Technique", *Int. J Ambient Energy*. Vol. 43, p.3518-3535, 2020, https://doi.org/10.1080/01430750.2020.1839550.

[28] R. K. Khadanga, A. Kumar, and S. Panda, "A Novel Modified Whale Optimization Algorithm for Load Frequency Controller Design of a Two-Area Power System

Composing of PV Grid and Thermal Generator", *Neural Computing and Applications*, 2020, Vol. 32, pp.8205-8216, https://doi.org/10.1007/s00521-019-04321-7.

[29] A. Kumar, and S. Suhag, "Whale Optimization Algorithm Optimized Fuzzy-PID Plus PID Hybrid Controller for Frequency Regulation in Hybrid Power System", *J. Inst. Eng. India Ser. B,* April 2022, Vol. 103, No. 2, pp. 633-648, http://dx.doi.org/10.1007/s40031-021-00656-9.

[30] Ö. Can, H. Eroğlu, and A. Öztürk, "The Automatic Generation Controller based on Whale Optimization Algorithm in PV-Thermal Power Systems", *Journal of the Faculty of Engineering and Architecture of Gazi University*, Vol. 38, No. 2, 2023, pp. 915-926, DOI: 10.17341/gazimmfd.984019.

[31] S. Kaur, L. K. Awasthi, A. L. Sangal, and G. Dhiman, "Tunicate Swarm Algorithm: A New Bio-Inspired based Metaheuristic Paradigm for Global Optimization", *Engineering Applications of Artificial Intelligence*, Vol. 90, April 2020, 103541, https://doi.org/10.1016/j.engappai.2020.103541.

[32] W. Aribowo, S. Muslim, B. Suprianto, S. I. Haryudo, Joko, "Tunicate Swarm Algorithm-Neural Network for Adaptive Power System Stabilizer Parameter", *Science & Technology Asia*, Vol.26, No.3, July-September 2021, pp.50-63, [Online]. https://ph02.tci-thaijo.org/index.php/SciTechAsia/article/view/241788 (Accessed Date: December 15, 2024).

[33] A. Saad, I. Hegazy, and E. M. El-Horbaty, "Tunicate Swarm Based Clustering and Routing Algorithm for Internet of Things", *International Journal of Intelligent Computing and Information Sciences*, Vol.23, No.1, 2023, pp.53-68, DOI: 10.21608 /ijicis.2023.175550. 1228.

[34] K. Lavanya, A. Mahendran, R. Selvanambi, M. Mazzara and J. D Hemanth, "Tunicate Swarm Algorithm with Deep Learning Based Land Use and Cover Change Detection in Nallamalla Forest India", *Appl. Sci.* 2023, 13, 1173. https:// doi.org/10.3390/app13021173.

[35] C. Du and J. Zhang, "An Enhanced Tunicate Swarm Algorithm with Symmetric Cooperative Swarms for Training Feedforward Neural Networks", *Symmetry* 2024, Vol. *16, No.* 7, 866, https://doi.org/10.3390/sym16070866.

[36] F. T. Tomy and R. Prakash, "Load Frequency Control of a Two Area Hybrid System Consisting of a Grid Connected PV System and Thermal Generator", *Int. J. of Research in Engineering and Technology*, Vol. 3, No. 7, May 2014, pp. 573-580, DOI: 10.15623/ijret.2014.0319103.

[37] C. Andic, S. Ozumcan, M. Varan and A. Ozturk, "A Novel Sea Horse Optimizer Based Load Frequency Controller for Two-Area Power System with PV and Thermal Units", 14 April 2023, https://doi.org/10.20944/preprints202304.0368.v1.

Contribution of Individual Authors to the Creation of a Scientific Article (Ghostwriting Policy)

Sahar M. Abd Elazim completed this paper in its entirety.

Sources of Funding for Research Presented in a Scientific Article or Scientific Article Itself

This study was conducted without any funding support.

Conflict of Interest

The author confirms the absence of any conflicts of interest.

APPENDIX

The network parameters are given as follows:

a) The constants of the heat grid: T_d =20 sec; T_{tu} =0.3 sec; T_{re} =10 sec;T_{12}=0.545 p.u; T_{go} =0.08 sec; K_d =120. Hz/p.u MW; B=0.80 p.u MW/Hz; a_{12}=-1; R =0.40 Hz/p.u MW; K_{re} =0.33 p.u MW.

b) The constants of TSA: Population of Tunicate =50, Maximum number of iterations =100, higher and lower span [-0.5, 0.5].

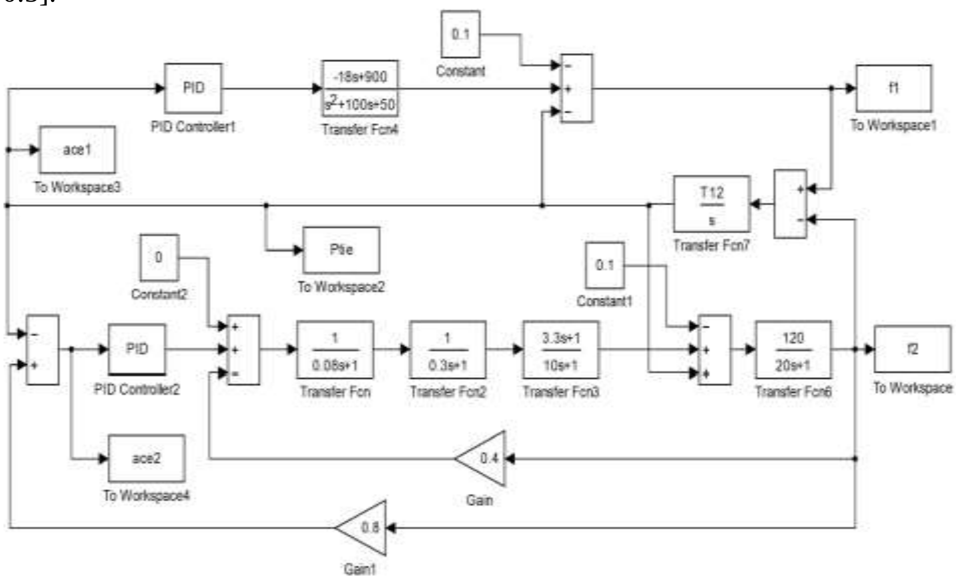

Fig. 2: The diagram of the analysed network

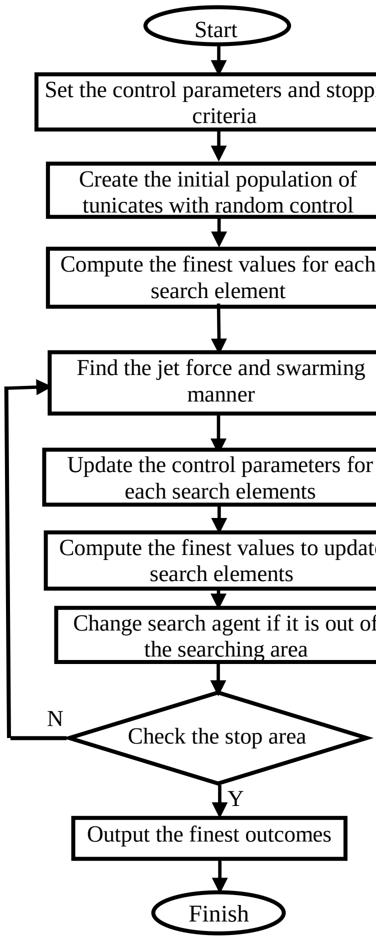

Fig. 3: Flowchart of TSA